Advances in Engineering Research, volume 198
International Seminar of Science and Applied Technology (ISSAT 2020)

High Performance Supercapacitor Based on Activated Carbon Electrodes Prepared Using Microwave Temperature as Process Parameter

Adekunle Moshood Abioye[1*] and Farid Nasir Ani[2]

[1]*Department of Mechanical/Production Engineering, Abubakar Tafawa Balewa University, Bauchi, Nigeria*
[2]*School of Mechanical Engineering, Faculty of Engineering, Universiti Teknologi Malaysia, UTM, 81310 Johor Bahru, Johor, Malaysia*
[*]*Corresponding author. Email: amadekunle@atbu.edu.ng*

ABSTRACT
The activated carbon (AC) electrodes were prepared by a two-step microwave-induced CO_2 activation of OPS using bed temperature as control parameter. The electrochemical properties of the AC electrodes were investigated at room temperature by cyclic voltammetry (CV), galvanostatic charge-discharge (GCD) and electrochemical impedance spectroscopy (EIS) in 1 M H_2SO_4. The morphology, textural and chemical composition of the AC electrodes were characterized using scanning electron microscopy (SEM), transmission electron microscopy (TEM), N_2 adsorption isotherm and X-ray diffraction (XRD). The specific surface area (S_{BET}), the total pore volume (V_t) and the micropore volume (V_μ) were found to increase with increase in both bed temperature and activation time with AC900-40 having the highest BET surface area of 574.37 $m^2\ g^{-1}$, total pore volume of 0.124 $cm^3\ g^{-1}$ and micropore volume of 0.116 $cm^3\ g^{-1}$. However, activation time was observed to have more profound effect as indicated by the values for AC800-40 being higher than that of AC900-20. The results of the electrochemical characterization show that the AC electrodes exhibit specific capacitance, power density and energy density of 134.68 F g^{-1}, 225 W kg^{-1} and 4.68 Wh Kg^{-1}, respectively. Thus, the results indicated that using bed temperature as control parameter in microwave heating is a promising route to producing AC electrode with excellent performance.
Keywords: *Oil palm shell, activated carbon, microwave activation, supercapacitor*

1. INTRODUCTION

Solar and wind energy are two of the renewable energy sources with abundant natural supply capable of meeting the global energy demand. However, the intermittent nature of these energy sources demands the provision of an energy storage system for smoothing of the energy being generated and storage of the excess energy during peak period for use during the off-peak period.

Batteries, supercapacitors and fuel cells belong to the system of electrochemical energy storage that form an integral part of renewable energy group. Although, the battery is the number one choice as storage device, nonetheless, much attention is currently being paid to supercapacitors due to high power density that is in multifold of that of batteries, high specific capacitance and extended cycle life [1]. Furthermore, supercapacitors are safe and almost maintenance free thus presenting a practical way out to energy problem in rural areas that are not connected to public grids [2]. A major challenge confronting the supercapacitors is the small energy density. To increase the energy density of supercapacitor there must be a corresponding increase in either the specific capacitance or potential window or both, since the energy density of the capacitor has a direct proportionality to the specific capacitance and square of the voltage. Addressing the problem require the use of electrode materials with high specific capacitance, electrolytes with wide voltage range and optimization of the structure of integrated system [2]. The electrochemical characteristics and behavior of supercapacitors are largely dependent on the electrode material used for their fabrication. The electrical double layer capacitors (EDLCs) are fabricated using carbon based electrode materials such activated carbon. The pseudocapacitors on the other hand are fabricated using either transition metal oxide or conducting polymer.

Activated carbons (AC) are usually prepared using physical or chemical activation process. Physical activation technique consists of the carbonization of the forerunner to obtain char and subsequent activation of the char using steam, carbon dioxide or air or a blend of these gasses as the activation agent [3]. Chemical activation technique on the other hand involves mixing of any

suitable activation/dehydration agents (e.g. $ZnCl_2$, H_3PO_4, KOH, K_2CO_3, NaOH) with either the carbonaceous material or biochar prior to activation. Thermal (conventional) and microwave heating are the two types of heating method usually employed to produce activated carbon. In thermal heating, carbonization and activation are commonly carried out in a tubular furnace which serves as the external heating source. Poor quality of the prepared activated carbon due to the thermal gradient from the surface to the interior of the particle and longer processing time are the bane of the conventional heating method. The increase in the use of microwave heating for the preparation of activated carbon by researchers currently being witness has been attributed to its shorter processing time and improved efficiency [4]. In microwave heating process, the heating is both internal and volumetric resulting in a rapid increase in the particle temperature which is uniformly propagated from the interior of the particle to the outer part of the particle [5]. Over the years, researchers in the area of microwave-induced preparation of activated carbons have used microwave power as a control parameter because, according to Guo and Lua [6], accurate measurement of the sample's temperature in the microwave energy field is practically not possible. This study is aimed at preparing activated carbon from oil palm shell via microwave-assisted CO_2 activation using bed temperature as process parameter for application as supercapacitor electrode.

2. METHODOLOGY

2.1. Production of Activated Carbon

Production of AC was carried out under microwave irradiation by physical activation that involved the carbonization of OPS to obtain biochar and subsequent activation of the biochar using CO_2 as activation agent. Modified domestic microwave (2.45GHz, IkW) having a power of 800W was used for this study. The bed temperature of the char and AC was monitored and controlled using a PID controller that was equipped with a K-type thermocouple. Details of the microwave-induced carbonization and CO_2 activation adopted for the fabrication of the AC can be found in our earlier study [7]. The four AC samples were termed AC800-20, AC900-20, AC800-40 and AC900-40, where 800, 900 stand for bed temperature in degree Celsius and 20, 40 stand for activation time in minutes.

2.2. Physicochemical Characterizations

The morphological and structural characterizations of the AC sample were done by scanning electron microscopy (SEM) analysis (Philip XL40) and transmission electron micrograph (TEM) analysis (JEM-ARM200F). Pore structure analysis of the AC samples was carried out using N_2 adsorption/desorption isotherm at -196 ^oC with Micromeritics 3Flex (Version 3.01). Data from the N_2 adsorption isotherm were fitted into Brunauer-Emmett-Teller (BET) equation for the estimation of the specific surface area. Measurement of the crystal phase was performed by X-ray diffraction (XRD) (Rigaku diffractometer) under Cu K_β radiation at 40 kV, 30 mA in the 2θ range of 20^o to 90^o.

2.2. Electrochemical Characterizations

Evaluation of the electrochemical properties of the as prepared electrode was carried out using a symmetrical supercapacitor cell having two identical electrode because of its ability to mimic practical supercapacitor. About 0.12 g of AC powder and 0.09 g of glycerin gel were mixed together and properly stirred to form an extrudable mass. Nickel foam with a thickness of 0.5 mm and 110 PPI was used as current collector and a 10 metric ton hydraulic press was used to compress the extrudable mass onto the nickel foam to form pellet having a thickness and diameter of about 0.7 mm and 20 mm, respectively. A 30 µm thick cellulose paper soaked in 1 M H_2SO_4 electrolyte was used as porous separator separating the two electrodes. The electrochemical tests were performed by cyclic voltammetry (CV), galvanostatic charge/discharge (GCD) and electrochemical impedance spectroscopy (EIS) on a Gamry Instrument (Interface 1000) at room temperature.

3. RESULTS AND DISCUSSION

3.1. Morphological Characteristics and Structural Analysis

The image from SEM exhibits pores and cavities of various sizes and shapes indicating a mixture of micropores and mesopores as depicted in Figure 1(a). As can be seen from Figure 1(a), micropores are more predominant. A major requirement for application of activated carbon as electrode material is a good pore size distribution. Figure 1(b) shows the parallelism of graphene layers that are associated with a graphitizable carbon and the 3D lace-work which is structure in activated carbons [8]. The N_2 adsorption/desorption isotherms obtained are shown in Figure 1(c). All the AC samples exhibit a Type I (reversible) isotherm of the IUPAC classification of physisorption isotherms. As can be seen from Figure 1(c), there is a steep uptake at low P/Po for all the samples. This steep uptake can be attributed to improved adsorbent-adsorptive interactions in narrow micropores, thus signifying that the Ac samples are predominantly microporous. Table 1 displays the characteristics of the AC samples. The data depicted in the table indicated that the specific surface area (S_{BET}), the total pore volume (V_t) and the micropore volume (V_μ) all increased with increase in both activation time and bed temperature with AC900-40 having the highest values. However, activation time was observed to have more profound effect as indicated by the values for AC800-40 being higher than that of AC900-20. Activated carbon yield is one of the criteria for commercial viability, however, since there is no significant difference in the AC yield, the preparation conditions for AC900-40 was taken as the optimum preparation conditions and AC900-40 was used for other

analysis. The XRD curve of the AC900-40 depicted in Figure 1(d) shows broad diffraction peaks with low crystallinity indicating that the AC is in an amorphous state. The in-plane conductivity requirement of activated carbon for electrochemical application is indicated by the peak at 23°, which is ascribed to (002) graphitic plane.

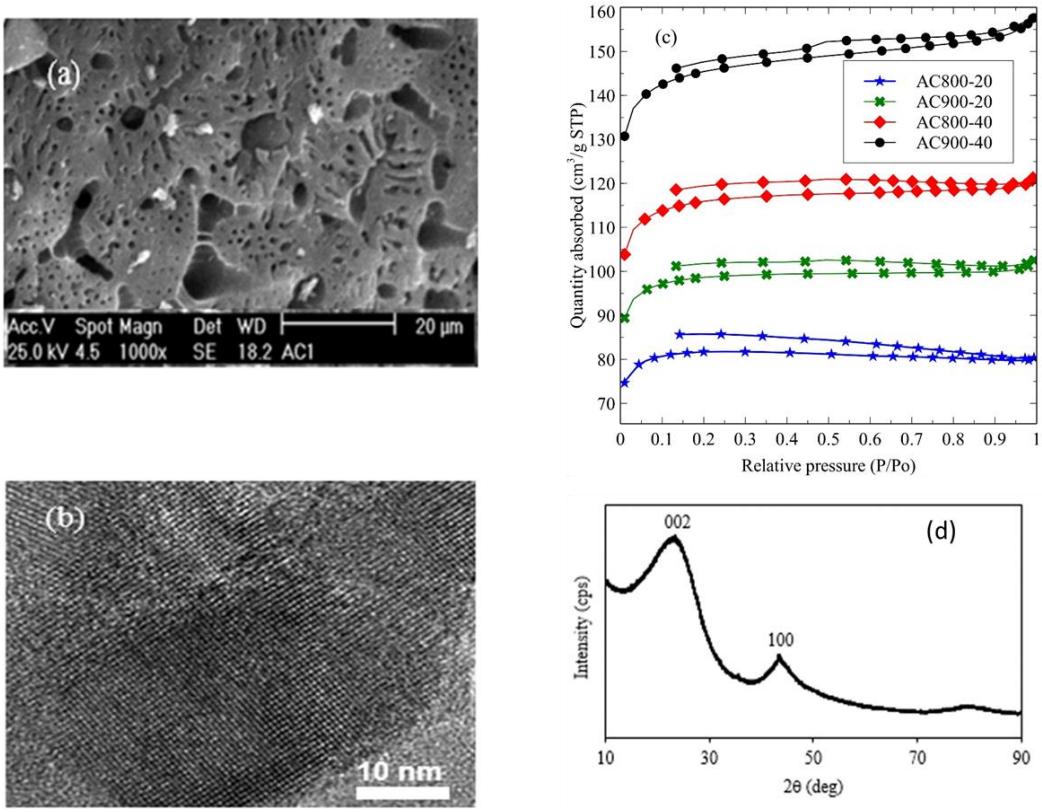

Figure 1 (a) SEM micrograph and (b) TEM image of AC900-40, (c) N_2 adsorption/desorption isotherms of all the ACs at -196 °C and (d) XRD curve of AC900-40

Table 1 Characteristics of the AC samples [7]

Sample	Temp (°C)	Time (min)	S_{BET} (m²/g)	V_t (cm³/g)	V_μ (cm³/g)	yield (%)
AC800-20	800	20	326.68	0.124	0.116	74.34
AC900-20	900	20	379.81	0.147	0.131	74.60
AC800-40	800	40	465.99	0.183	0.161	71.86
AC900-40	900	40	574.37	0.244	0.198	74.06

3.2. Electrochemical Characteristics

The storage mechanism of charges in the constructed supercapacitor was studied using cyclic voltammetry. The CV curves of the AC900-40 electrode at scan rate of 2, 5 and 10 mV s^{-1} are presented in Figure 2(a). The shape of the CV curves are similar and nearly symmetrical but slightly distorted from the normal CV shape of electrochemical double-layer capacitor. The distortion from classic shape of EDLC could be attributed to pseudocapacitance caused by the quasi-reversible surface reactions and the limitation in the charge transfer imposed by the narrow micropores [9]. The estimation of the static specific capacitance from the cyclic voltammogram was carried out using the following equation:

$$SC_{CV} = \left[\frac{1}{v(V_2-V_1)}\int_{V_1}^{V_2} I(V)dV\right] \times \frac{4}{m} \quad (1)$$

where V_1 and V_2 stand for lower and upper integral limits of the CV curve and I (V) represents the voltammetric current.

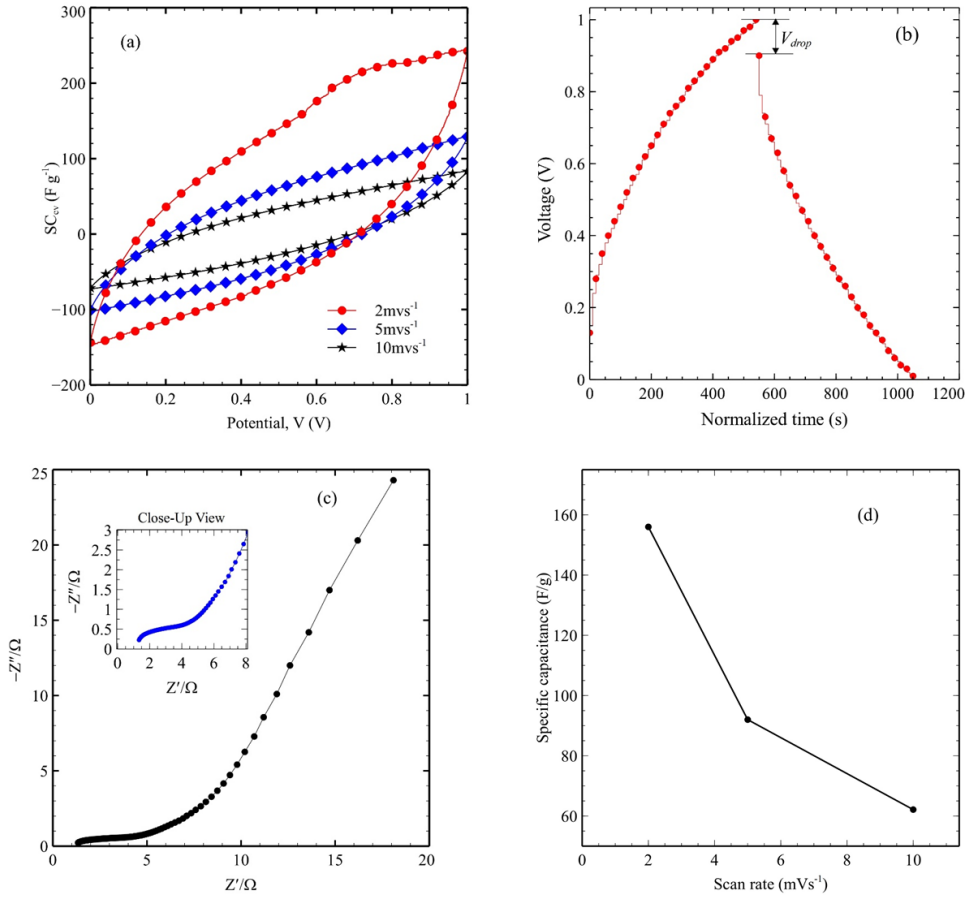

Figure 2 (a) CV at different scan rate, (b) GCD plot, (c) Nyquist plot and (d) specific capacitance at different scan rate of the AC900-40

The graph of specific capacitance against scan rate for AC900-40 is depicted in Figure 2(d). As can be seen in the graph there is a substantial drop in the specific capacitance from 156.00 F g^{-1} at 2 mV s^{-1} to about 60 F g^{-1} at 10 mV s^{-1}, thus signifying that when the scan rate was increased there was a significant decrease in the specific capacitance. The observed phenomenon is attributable to impaired diffusion within the pores of the AC electrodes [9], since the as prepared AC electrode was predominantly microporous.

The galvanostatic measurement of the supercapacitor cell was carried out at constant current of 10 mA. The voltage response from GCD test is shown in Figure 2(b). The GCD curve exhibits a triangular shape that is almost linear and symmetrical. Specific capacitance value of 134.68 F g^{-1} was obtained by the following equation:

$$SC_{\mathrm{g}} = \frac{I_d}{(\Delta V/\Delta t)} \times \frac{4}{m} \quad (2)$$

where I_d stands for discharge current, $\Delta V/\Delta t$ stands for discharging curve's gradient and m for total mass of the electrode material. Although, the SC_{g} fell short of SC_{CV}, however, the GCD is a more reliable method for the evaluation of the electrochemical performance of a practical supercapacitor cell. A key factor governing the performance of supercapacitor is the voltage drop (V_{drop}) corresponding to the equivalent series resistance, ESR_{g} (Ω) of the supercapacitor. The relationship between the V_{drop} and ESR_{g} is given by eqn. 3 in accordance with Ohm's law.

$$ESR_{\mathrm{g}} = \frac{V_{drop}}{\Delta I} \quad (3)$$

where ΔI is the current at the point of changing from charging to discharging.

From the galvanostatic charge-discharge measurement results the estimation of power density P (W/kg) was based on eqn. 4 while the estimation of energy density E (Wh/kg) was based on eqn. 5.

$$P = \frac{V^2}{4ESR_g} \times \frac{1000}{m} \quad (4)$$

$$E = \frac{1}{2}CV^2 \times \frac{1}{36 \times m} \quad (5)$$

where V (V) represents the operating voltage window (exclusive of the voltage drop), C (F) represents the supercapacitor capacitance and m (g) represents the total

mass of the electrode material. The V_{drop} value and the corresponding ESR_g value were determined to be 0.100 and 5.0 Ω, respectively. At power density of 225.0 W kg^{-1}, the AC900-40 electrode exhibits a practical energy density of 4.68 Wh kg^{-1}.

The electrochemical impedance of the supercapacitor was demonstrated using Nyquist plot as shown in Figure 2(c). According to Figure 2(c), at the high frequency region the supercapacitor exhibits a small semicircle while at the low frequency region the supercapacitor exhibits near vertical line showing that the supercapacitor impedance behavior is near ideal electrochemical impedance behavior. The specific capacitance (SC_{eis}) of the supercapacitor was found to be 130.94 F g^{-1} using the following equation:

$$SC_{eis} = \frac{1}{2\pi f Z''} \times \frac{4}{m} \quad (6)$$

where f stands for frequency (0.001 Hz), Z'' stands for imaginary part of the impedance curve and m (g) stands for total mass of the electrode material.

The specific capacitance achieved in this study is comparable to those reported in literature and in some cases [10] even higher than the reported value as shown in Table 2. As may be observed in Table 2, there are cases where there is correlation between the surface area and the performance of the AC, thus signifying that there other factors affecting the performance of the supercapacitor in addition to the surface area of the AC. These factors include among others the precursor material, the characteristics of the AC such as pore structure and surface functional groups and the interaction between the electrolyte and electrode at the electrode/electrolyte interface.

Table 2 Comparison of S_{BET} and specific capacitance (SC) of some porous carbons reported in literature

Biomass precursor	Activating Method	Electrolyte	S_{BET} (m^2 g^{-1})	SC (F g^{-1})	Reference
Oil Palm Shell	MW-CO_2	1 M H_2SO_4	574.37	156	This study
Papaya seeds	$ZnCl_2$	1 M H_2SO_4	1213	472	[11]
Laver (seaweed)	Carbonization	6 M KOH	≤ 2	116.9	[12]
Coconut shell	KOH	PVdF(HFP)-PMMA-NaSCN	1640	356.2	[13]
Cow dung	KOH	1 M Et_4NBF_4	1984	124	[14]
Rice Husks	MW-$ZnCl_2$	1 M Et_4NBF_4/PC	1527	194	[15]
Peanut shell	MW-$ZnCl_2$	1 M Et_4NBF_4/PC	1552	199	[15]
Oil palm EFB	KOH+CO_2	1 M H_2SO_4	1704	149	[9]
Sugarcane bagasse	MW-$ZnCl_2$	$EMImBF_4$	1416	138	[16]
Cassava peel waste	KOH+CO_2	0.5 M H_2SO_4	1352	153	[17]
Sugarcane bagasse	$ZnCl_2$	1 M H_2SO_4	1788	300	[18]
Apricot shell	NaOH	6 M NaOH	2335	339	[19]
Corn grains	KOH	6 M KOH	3199	257	[20]
Oil Palm Kernel Shell	Physical-Steam	1 M H_2SO_4	730	74.76	[10]

4. CONCLUSION

This study have shown that activated carbon electrode with high specific capacitance and power density can be produced using controlled bed temperature as process parameter. The BET surface area, which is an important determinant of AC electrode performance was found to vary directly with bed temperature and activation time, suggesting that a good control of the bed temperature could result in AC electrodes with superior electrochemical performance.

REFERENCES

[1] A.M. Abioye, F.N. Ani, Recent development in the production of activated carbon electrodes from agricultural waste biomass for supercapacitors: A review, Renewable and Sustainable Energy Reviews, 52 (2015), 1282-93. DOI: http://dx.doi.org/10.1016/j.rser.2015.07.129

[2] Poonam, K. Sharma, A. Arora, S.K. Tripathi, Review of supercapacitors: Materials and devices, Journal of Energy Storage, 21 (2019), 801-25. DOI: https://doi.org/10.1016/j.est.2019.01.010

[3] T. Yang, A.C. Lua, Characteristics of activated carbons prepared from pistachio-nut shells by physical activation, Journal of Colloid and Interface Science, 267 (2) (2003), 408-17. DOI: http://dx.doi.org/10.1016/S0021-9797(03)00689-1

[4] J.A. Menéndez, A. Arenillas, B. Fidalgo, Y. Fernández, L. Zubizarreta, E.G. Calvo, J.M. Bermúdez, Microwave heating processes involving carbon materials, Fuel Processing Technology, 91 (1) (2010), 1-8. DOI: https://doi.org/10.1016/j.fuproc.2009.08.021

[5] Q.-S. Liu, T. Zheng, N. Li, P. Wang, G. Abulikemu, Modification of bamboo-based activated carbon using microwave radiation and its effects on the adsorption of methylene blue, Applied Surface Science, 256 (10) (2010), 3309-15. DOI: https://doi.org/10.1016/j.apsusc.2009.12.025

[6] J. Guo, A.C. Lua, Preparation of activated carbons from oil-palm-stone chars by microwave-induced carbon dioxide activation, Carbon, 38 (2000), 1985-93. DOI: http://dx.doi.org/10.1016/S0008-6223(00)00046-4

[7] A.M. Abioye, L.N. Abdulkadir, F.N. Ani. CO_2 activated carbon from oil palm shell using microwave temperature as process parameter. IET Conference Proceedings [Internet]. 2018:[1-4 pp.]. Available from: https://digital-library.theiet.org/content/conferences/10.1049/cp.2018.1522.

[8] H. Marsh, F. Rodríguez-Reinoso. SEM and TEM Images of Structures in Activated Carbons. Activated Carbon. Oxford: Elsevier Science Ltd; 2006. p. 366-82.

[9] R. Farma, M. Deraman, A. Awitdrus, I.A. Talib, E. Taer, N.H. Basri, J.G. Manjunatha, M.M. Ishak, B.N. Dollah, S.A. Hashmi, Preparation of highly porous binderless activated carbon electrodes from fibres of oil palm empty fruit bunches for application in supercapacitors, Bioresour Technol, 132 (2013), 254-61. DOI: http://dx.doi.org/10.1016/j.biortech.2013.01.044

[10] I.I. Misnon, N.K.M. Zain, R. Jose, Conversion of Oil Palm Kernel Shell Biomass to Activated Carbon for Supercapacitor Electrode Application, Waste and Biomass Valorization, 10 (6) (2019), 1731-40. DOI: https://doi.org/10.1007/s12649-018-0196-y

[11] P. Kalyani, A. Anitha, A. Darchen, Obtaining Activated Carbon from Papaya Seeds for Energy Storage Devices, International Journal of Engineering Sciences & Research Technology, 4 (1) (2015), 110-22.

[12] X. Wu, W. Xing, J. Florek, J. Zhou, G. Wang, S. Zhuo, Q. Xue, Z. Yan, F. Kleitz, On the origin of the high capacitance of carbon derived from seaweed with an apparently low surface area, J Mater Chem A, 2 (44) (2014), 18998-9004. DOI: https://doi.org/10.1039/c4ta03430a

[13] A. Jain, S.K. Tripathi, Fabrication and characterization of energy storing supercapacitor devices using coconut shell based activated charcoal electrode, Materials Science and Engineering: B, 183 (2014), 54-60. DOI: http://dx.doi.org/10.1016/j.mseb.2013.12.004

[14] D. Bhattacharjya, J.-S. Yu, Activated carbon made from cow dung as electrode material for electrochemical double layer capacitor, Journal of Power Sources, 262 (2014), 224-31. DOI: http://dx.doi.org/10.1016/j.jpowsour.2014.03.143

[15] X. He, P. Ling, J. Qiu, M. Yu, X. Zhang, C. Yu, M. Zheng, Efficient preparation of biomass-based mesoporous carbons for supercapacitors with both high energy density and high power density, Journal of Power Sources, 240 (2013), 109-13. DOI: 10.1016/j.jpowsour.2013.03.174

[16] W.-J. Si, X.-Z. Wu, W. Xing, J. Zhou, S.-P. Zhuo, Bagasse-based Nanoporous Carbon for Supercapacitor Application, Journal of Inorganic Materials, 26 (1) (2011), 107-12. DOI: https://doi.org/10.3724/SP.J.1077.2010.10376

[17] A.E. Ismanto, S. Wang, F.E. Soetaredjo, S. Ismadji, Preparation of capacitor's electrode from cassava peel waste, Bioresour Technol, 101 (10) (2010), 3534-40. DOI: 10.1016/j.biortech.2009.12.123

[18] T.E. Rufford, D. Hulicova-Jurcakova, K. Khosla, Z. Zhu, G.Q. Lu, Microstructure and electrochemical double-layer capacitance of carbon electrodes prepared by zinc chloride activation of sugar cane bagasse, Journal of Power Sources, 195 (3) (2010), 912-8. DOI: 10.1016/j.jpowsour.2009.08.048

[19] B. Xu, Y. Chen, G. Wei, G. Cao, H. Zhang, Y. Yang, Activated carbon with high capacitance prepared by NaOH activation for supercapacitors, Materials Chemistry and Physics, 124 (1) (2010), 504-9. DOI: 10.1016/j.matchemphys.2010.07.002

[20] M.S. Balathanigaimani, W.-G. Shim, M.-J. Lee, C. Kim, J.-W. Lee, H. Moon, Highly porous electrodes from novel corn grains-based activated carbons for electrical double layer capacitors, Electrochemistry Communications, 10 (6) (2008), 868-71. DOI: http://dx.doi.org/10.1016/j.elecom.2008.04.003